PCCP

Time-resolved dual fluorescence of 1-phenylpyrrole in acetonitrile: molecular dynamics simulations of solvent response to twisted intramolecular charge transfer

Jörn Manz,[a] Boris Proppe[b] and Burkhard Schmidt*[c]

[a] *Institut für Chemie—Physikalische und Theoretische Chemie, Freie Universität Berlin, Takustr. 3, D-14195 Berlin, Germany*
[b] *Zentraleinrichtung für Datenverarbeitung, Freie Universität Berlin, Fabeckstr. 32, D-14195 Berlin, Germany*
[c] *Institut für Mathematik II, Freie Universität Berlin, Arnimallee 2–6, D-14195 Berlin, Germany. E-mail: burkhard@math.fu-berlin.de*

Received 18th October 2001, Accepted 31st January 2002
First published as an Advance Article on the web 10th April 2002

The real-time dynamics of solvation of 1-phenylpyrrole (PhPy) in acetonitrile (ACN) upon electronic excitation is investigated by means of non-equilibrium molecular dynamics simulations. The interaction is modeled by empirical intermolecular pair potentials using partial charges and intramolecular torsional potentials from high level *ab initio* calculations of ground and excited states of PhPy. The intramolecular torsional motion following sudden excitation from the twisted ground state to the 2 ^{1}B charge transfer state is strongly damped by the viscous ACN solvent, leading to a near-exponential approach of the perpendicular conformation on a timescale of about 5–10 ps. The intermolecular dynamics is characterized by rapid reorientation of the solvent molecules on a timescale of 100 fs followed by weak quasi-coherent librations. The solvatochromic red-shift of the charge transfer state with respect to the locally excited 1 ^{1}B state results in dual fluorescence, thus supporting the twisted intramolecular charge transfer (TICT) mechanism for PhPy in a polar solvent.

1 Introduction

The understanding of photophysical or photochemical processes in electronically excited molecules in solution presents a challenging problem.[1] On the one hand, the electronic structure of excited states is rather complex because of the high degree of electron correlation. On the other hand, the solute–solvent interaction becomes particularly important when charges are transferred, *e.g.* in intramolecular electron or proton transfer processes. The former manifests itself in the phenomenon of dual fluorescence, *i.e.* the occurrence of two distinct fluorescence bands, which is found for a large class of organic donor-acceptor compounds in polar solution. Compared to "normal" fluorescence bands, which are due to local excitation (LE) in either the donor or acceptor moiety, "anomalous" fluorescence bands exhibit a characteristic Stokes shift. It is attributed to an intramolecular charge transfer (CT) in certain electronically excited states accompanied by a significant molecular rearrangement. Hence, the different minimum energy molecular conformation of ground and CT state causes the frequency shift between the two emission bands. The timescale of the buildup of dual fluorescence is connected with the dynamics of the intramolecular rearrangement. In a certain class of donor-acceptor compounds the dominant internal mode promoting the charge transfer is the torsion of the two moieties about the single bond connecting them. This phenomenon is commonly referred to as twisted intramolecular charge transfer (TICT).[2,3,4]

Another contribution to dual fluorescence and the corresponding Stokes shift is the solvatochromic effect. It originates from the solvent response to a charge transfer within the solute molecule. Driven by the long range polar forces, the solvent molecules respond to the change in the charge distribution by reorienting themselves. Usually the CT state is more polar than the ground state and the stabilization of the former leads to a bathochromic shift of the anomalous emission with respect to the normal emission ("red-shift") which increases with the solvent polarity. If the excitation of the solute particle to the CT state is induced instantaneously, *e.g.* by ultrafast laser pulses, the dual fluorescence can be monitored in real time.[5] Hence, dynamic Stokes shifts offer a molecular view of solvation dynamics upon CT within a solute molecule. In principle, the solvation dynamics can be characterized as follows:[6–10] (1) A purely inertial motion of the solvent particles leads to a Gaussian increase of the Stokes shift. (2) A collective vibrational/librational motion of the solvent particles may give rise to oscillations of the dynamic Stokes shift. Typically, such oscillations die out quickly due to the effect of dissipation. (3) On a much longer timescale "diffusive" processes involve restructuring of the solvent environment.

In the present work we investigate the dual fluorescence and the corresponding solute–solvent dynamics of a molecule upon excitation to a TICT state. The main emphasis will be on the time dependence of the Stokes shift. In particular, the timescale of the two contributions to the frequency shift will be compared. These are the conformational rearrangement, *i.e.* the intramolecular twist, and the solvent reorientation, respectively. The system to be investigated is 1-phenylpyrrole (PhPy) dissolved in acetonitrile (ACN), which is motivated by several reasons: First of all, PhPy is one of the simplest donor-acceptor compounds for which TICT has been identified both in experiment [11–13] and in high level CASSCF/CASPT2 *ab initio*[14] and DFT/MRCI[15] calculations. Second, because of the simple structure of the PhPy molecule, and by analogy with

 DOI: 10.1039/b109488b

the related system 9-(*N*-carbazolyl)-anthracene,[16,17] the only mode promoting the CT is the torsion of donor and acceptor about the single bond connecting them. Note that for dimethylaminobenzonitrile (DMABN), which has served as a prototypical molecule in many studies, other competing intramolecular mechanisms have been discussed in refs. 18–20, which can, however, be excluded for PhPy. Finally, acetonitrile is the simplest aprotic polar solvent whose solvation dynamics has been studied extensively.[6–9]

The remainder of the paper is organized as follows. In Section 2 we propose our mixed quantum chemical/classical mechanical treatment of solvation dynamics. Our results for the intramolecular and intermolecular contributions to the time-dependent fluorescence spectra are presented in Section 3. Finally, our conclusions are given in Section 4.

2 Model

Our approach to simulate the dynamic Stokes shifts is similar to previous studies of CT states of DMABN in solution.[10,21] Instead of using reaction field methods which treat the solvent as a dielectric continuum (see *e.g.* ref. 14), we employ a microscopic picture to investigate the solvation dynamics. Because a supermolecular *ab initio* treatment of excited states is prohibitive even for a small number of solvent molecules, the potential energy function is constructed from high level *ab initio* results for the gas phase PhPy solute[14] augmented by empirical solvent-solute interactions. The latter are based on charge distributions for the different electronic states of the solute molecule which are extracted from the corresponding electronic wavefunctions. Based on this model, classical non-equilibrium molecular dynamics simulations of instantaneously excited PhPy in acetonitrile solution are carried out.

A. Electronic structure of PhPy

The electronic structure of the ground and the lowest few excited states of PhPy *in vacuo* has been thoroughly investigated in ref. 14. For reasons of completeness, we shall briefly report here the most important results. Using the MOLCAS-4 quantum chemistry software,[22] *ab initio* calculations accounting for electronic correlation by means of a multiconfigurational CASPT2 method have been performed. An ANO C,N[3s2p1d]/H[2s] basis set has been employed, and the active space has been constructed from 12 electrons in 11 π orbitals. Fixing all intra-ring degrees of freedom, wavefunctions and energies have been obtained as a function of the intramolecular torsional coordinate τ. Except for the special case of a coplanar ($\tau = 0°$) or perpendicular ($\tau = 90°$) conformation with C_{2v} symmetry, the molecule belongs to the C_2 point group, see Fig. 1.

The resulting ground state (GS) potential energy curve (1 ^{1}A) is shown in Fig. 2. In good agreement with experimental

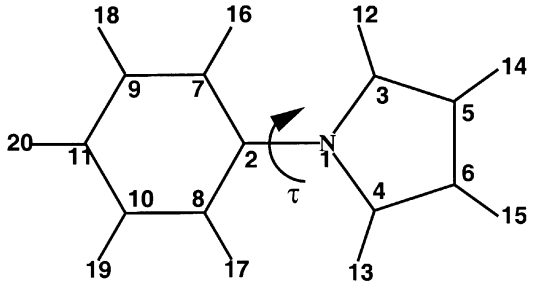

Fig. 1 Molecular structure of 1-phenylpyrrole. Note that the C_{2v} symmetry for planar ($\tau = 0°$) and perpendicular ($\tau = 90°$) conformation reduces to C_2 symmetry in the general case.

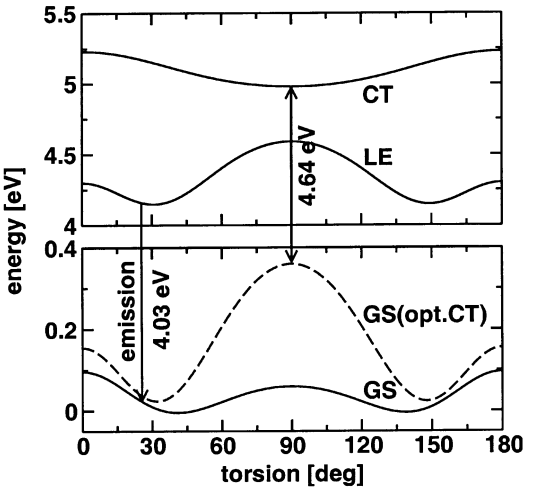

Fig. 2 Ground and excited state potential energy curves for the isolated PhPy molecule obtained from high level CASPT2 calculations *vs.* intramolecular twist angle for ground state (GS, 1 ^{1}A), locally excited state (LE, 1 ^{1}B) and charge transfer state (CT, 2 ^{1}B) after geometry optimization.[14] The dashed curve shows the results of GS calculations for the geometry optimized for the CT state.

work[13] and other calculations,[15] the most stable geometry is found to be twisted ($\tau = 41.4°$). Barrier heights of 0.101 and 0.064 eV for planar or perpendicular conformation have been obtained, respectively. The first electronically excited state (1 ^{1}B) corresponds to a local excitation (LE) mainly within the phenyl group with a minimum energy configuration at $\tau = 25.5°$. Although this state is hardly accessible in absorption spectroscopy due to its low oscillator strength, it has been identified as the source of "normal" fluorescence of twisted PhPy at 4.03 eV.[14] Its torsional dependence is also given in Fig. 2. Note that both the GS and LE state are characterized by relatively low dipole moments of -3 to -1 D (pyrrole more negative than phenyl group).

The second excited state (2 ^{1}A) carries most oscillator strength (not shown in the figure). The calculated absorption frequency (5.07 eV) is in good agreement with recent experiments.[13] It may be speculated that upon excitation of this state population is "funneled" into the first excited state through a conical intersection.[1,23] The third excited state (2 ^{1}B) involves a charge transfer (CT) from the pyrrole to the phenyl group with small oscillator strength, and with a perpendicular minimum energy configuration ($\tau = 90°$). The molecular dipole moment increases strongly with the intramolecular twist from +6.6 D ($\tau = 0°$) to +11.0 D ($\tau = 90°$), thus indicating a twisted intramolecular charge transfer (TICT) mechanism. The corresponding vertical emission for perpendicular PhPy is calculated as the difference of CT and GS potential energy both calculated for the optimized geometry of the CT state. The corresponding energy difference of 4.64 eV is blue-shifted against the LE emission at 4.03 eV mentioned above. These results for isolated PhPy serve as a reference for the investigation of PhPy in solution. As already suggested by reaction field *ab initio* calculations,[14] the very polar TICT state is stabilized in a polar solvent leading to a red-shifted "anomalous" fluorescence as will be shown below in detail.

B. Interaction between PhPy and ACN

In order to obtain the total potential energy of a solute–solvent system, the intramolecular twisting potentials for PhPy are augmented by solute–solvent and solvent–solvent interactions. We follow the standard force field approach using pairwise additive potentials for the intermolecular interactions where

each atom is described as one site with the exception of the methyl group of ACN which is treated as a "united atom". The pair interactions are expressed as a sum of two contributions.

First, the short-range repulsion and the van der Waals attraction are described by a Lennard–Jones potential. We resort to Jorgensen's optimized potentials for liquid simulations (OPLS) model, adapting parameters for PhPy[24] and ACN.[25] Although this force field was originally developed for the electronic ground state, we use the parameters also as an approximate description of the excited states.

The second contribution to the pair potentials comes from the electrostatic interaction. While we resort to standard OPLS partial charges for ACN,[25] the use of Mullikan partial charges for PhPy extracted from the electronic wavefunctions allows us to account for the different charge distributions of the individual electronically excited states. Our results for the partial charges of PhPy are collected in Table 1. The reversal and the absolute change of the dipole moment upon excitation from the GS to the CT state indicate a transfer of −0.53 elementary charges from the pyrrole to the phenyl ring. This transfer is most apparent in the charges of nitrogen (N_1) and the phenyl carbon participating in the inter-ring bond (C_2). Furthermore, there are distinct changes in the charges of the CH groups at the *ortho* position of the pyrrole group. In contrast, the partial charges obtained for the locally excited (LE) state (not tabulated) are very similar to those for the ground state with the difference being less than 0.02 e for each of the atoms.

3 Non-equilibrium molecular dynamics

In this section we present results of classical non-equilibrium molecular dynamics simulations of PhPy dissolved in ACN for different electronic states of the solute molecule. In our simulations we consider a model of 237 ACN molecules solvating a single PhPy molecule employing periodic boundary conditions to simulate a bulk liquid.[26] Note that for the purpose of the present work the intra-ring vibrations as well as the internal ACN vibrations are not of interest. Furthermore, the fast oscillations would make the numerical integration of the equations of motion less efficient. Consequently we use constraint dynamics to "freeze" these degrees of freedom by means of the iterative RATTLE scheme[27] in some of the simulations. Other simulations were performed using the GROMACS molecular dynamics software[28] where the PhPy is completely flexible. Typically, a time step of 2 fs was employed.

Table 1 Partial charges of PhPy obtained from Mullikan analysis of the CASSCF wavefunctions for the ground state (GS, $\tau = 41.4°$) and the charge transfer state (CT, $\tau = 90°$). The indices of the atoms refer to Fig. 1

Atom	GS	CT
N_1	−0.24	−0.07
C_2	−0.00	−0.22
$C_{3(4)}$	−0.23	−0.13
$C_{5(6)}$	−0.29	−0.23
$C_{7(8)}$	−0.26	−0.33
$C_{9(10)}$	−0.22	−0.22
C_{11}	−0.24	−0.38
$H_{12(13)}$	0.29	0.35
$H_{14(15)}$	0.27	0.31
$H_{16(17)}$	0.29	0.23
$H_{18(19)}$	0.27	0.24
H_{20}	0.26	0.24

A Intramolecular torsional dynamics

In a first set of molecular dynamics simulation we investigate the intramolecular torsional dynamics of PhPy in acetonitrile and compare it with that of isolated PhPy. For this purpose we use torsional potentials for different electronic states obtained by fitting a power series in $\cos^2\tau$ to the *ab initio* results for selected values of the twisting angle τ. A set of initial conditions for ground state PhPy in ACN is generated for room temperatures (300 K) in the following way. Starting from a random initial condition, a molecular dynamics run is performed where the temperature is adjusted by scaling the velocities of the particles appropriately.[26] After that, the system is allowed to equilibrate for 60 ps. The subsequent equilibrium simulation with approximately constant temperature is used to generate a set of initial conditions by sampling 500 configurations.

In order to simulate the non-equilibrium dynamics following a sudden electronic excitation, both the torsional potential and the partial charges of PhPy were changed to mimic the CT state. Note that the charge distribution of the CT state for the twisted geometry ($\tau = 41.4°$) is quite similar to that for the perpendicular geometry (dipole moment of 8.5 D *vs.* 11.0 D). Hence, we used the partial charges of the latter and assumed them to be approximately constant during our MD simulations of the CT state torsional dynamics. Results for typical trajectories are shown in Fig. 3. First consider the torsional dynamics of PhPy in vacuum. Starting from the twisted minimum geometry ($\tau = 41.4°$), the molecule begins to undergo large-amplitude torsional vibrations around the perpendicular minimum energy configuration of the charge transfer state, with slow damping due to intramolecular vibrational energy redistribution (IVR). Due to the large moment of inertia and the relatively shallow potential energy curve the period of vibration is as long as 700 fs. The torsional dynamics for PhPy in ACN is entirely different. The PhPy molecule reaches the perpendicular conformation in a diffusion-like motion only after about 5–10 ps, *i.e.* the torsional motion behaves like an overdamped oscillator with a near-exponential approach of the perpendicular conformation. The fast quasi-random small-amplitude vibrations superimposed on that behavior are due to hard collisions of single solute molecules with one of the rings and reflect mainly the thermal motion of the solvent at $T = 300$ K. The merely solute-induced contribution to the solvent dynamics will be investigated in the following.

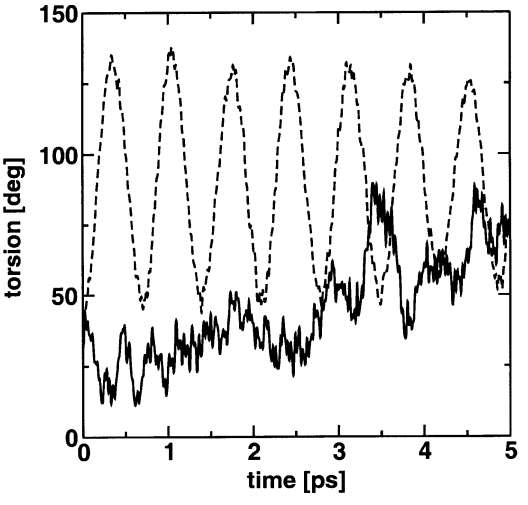

Fig. 3 Intramolecular dynamics of PhPy following instantaneous electronic excitation to the CT state. Dashed curve: isolated PhPy molecule. Solid curve: PhPy solvated in ACN ($T = 300$ K). See text for the details of the non-equilibrium molecular dynamics simulations.

B. Intermolecular solvation dynamics

In this section we focus our attention on the intermolecular dynamics of the ACN solvent upon electronic excitation of the PhPy solute to the LE and CT state and its effect on time-resolved fluorescence. In order to study the solvent response to the change in the charge distribution of the solute molecule independently of other dynamical effects, we perform the following simplified *Gedankenexperiment*. Upon absorption the second excited state ($2\ ^1A$) of the PhPy molecule has been populated. Subsequently, there has been a radiationless transition to either the LE or CT state which is correlated with intramolecular torsional motion towards the new minimum geometry of $\tau = 25.5°$ or $\tau = 90°$, respectively. This hypothetical initial state is assumed to remain constant for the duration of our simulation of time-resolved dual fluorescence of approximately 1 ps. On the one hand, this is supported by the above finding of relatively slow torsional dynamics. On the other hand, the results of previous reaction field *ab initio* calculations predict the "normal" (LE) and "anomalous" (TICT) fluorescence to originate from these conformations.[14] A more detailed study of the mentioned population transfer is beyond the scope of the present study. However, it may be speculated that the radiationless transition proceeds *via* a conical intersection of the respective potential energy surfaces.

The molecular dynamics simulations are organized in the following way. First, ground state ensembles of initial conditions are generated as described above but for the PhPy twisting degree of freedom fixed to $\tau = 25.5°$ or $\tau = 90°$. The initial velocities are set to zero in order to study the solvent rearrangement unperturbed by thermal motion. Then the partial charges are suddenly changed to those corresponding to the electronically excited LE or CT state. Subsequently, the solvation dynamics is monitored in time for the duration of 1 ps. A sensitive observable of the system evolving on the excited state potential energy surfaces is the time-dependent fluorescence spectrum. Assuming the electronic transition to the electronic ground state to be fast enough that the system configuration is left unchanged (vertical Franck–Condon transition), the emission frequencies for each trajectory are obtained as the difference between the total potential energy for the LE or CT state and the ground electronic state (GS) calculated for the same geometry[10]

$$\Delta E_{\mathrm{LE/CT}}(t) = H_{\mathrm{LE/CT}} + U_{\mathrm{LE/CT}} - (H_{\mathrm{GS}} + U_{\mathrm{GS}}). \qquad (1)$$

Here it is sufficient to consider only the solute intramolecular energy H and the solute–solvent interaction U because the solvent–solvent interaction is independent of the electronic state of the solute.

Simulated time evolutions of the distributions of the energy shifts defined in eqn. (1) are displayed as histograms in Fig. 4. For the LE state no notable evolution is observed. The distributions are confined to a relatively narrow energetic regime around the calculated emission frequency of 4.03 eV for isolated PhPy. In accordance with reaction field calculations, the solvatochromic shift of the LE state is negligible because of the very similar charge distribution of the GS and LE states.[14] In contrast, the solvent is reacting strongly to an excitation of PhPy (GS, $\tau = 90°$) to the polar CT state. Upon sudden excitation we observe the CT state energy to be centered around 5.05 eV ($t = 0$). The blue-shift with respect to the vacuum emission frequency at 4.64 eV indicates that the charge transfer is not compatible with the solvent environment equilibrated for the GS. Hence there is a strong impetus for rearrangement of the solvent ACN molecules. This can be observed in the histograms for later times: For $t = 100$ fs the mean value is already found at 4.27 eV. One picosecond after the excitation the spectrum is already almost stationary and should thus be comparable to a conventional fluorescence spectrum. With a band center at 3.87 eV, the contribution of the solvent response to the red-shift of the "anomalous" fluorescence amounts to $4.64 - 3.87 = 0.77$ eV. Thus the TICT emisson indeed becomes red-shifted *vs.* the LE emission because of the strong stabilization of the charge transfer state in a polar solvent. This is in reasonable agreement with the reaction field calculations published in ref. 14, yielding a shift of 0.92 eV. Moreover, the combined fluorescence of LE and CT state very closely resembles the experimental spectrum[11] reproduced in the lower part of Fig. 4. Its main peak and its low-energy shoulder can be attributed to normal (LE) and "anomalous" (CT) fluorescence, respectively.

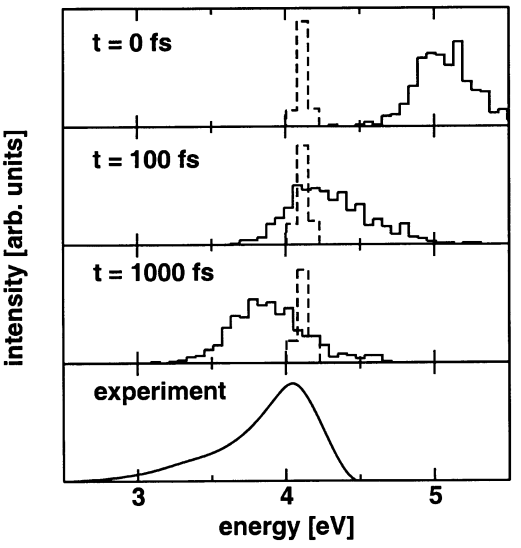

Fig. 4 Vertical LE–GS (dashed) and CT–GS (solid) energy differences for PhPy in ACN for selected times after instantaneous electronic excitation, see eqn. (1). Note that the LE and CT histograms are not normalized with respect to each other. In the limit of long times ($t = 1$ ps) the simulations compare well with the experimental fluorescence spectrum of ref. 11.

Apart from yielding stationary spectra in the limit of long times after the excitation process, the present simulations offer a detailed insight into the dynamics of the solvation dynamics. One way to characterize the solvent response upon CT excitation is to calculate the normalized Stokes shift (relaxation correlation function) defined by

$$S(t) = \frac{\langle \Delta E_{\mathrm{CT}}(t) \rangle - \langle \Delta E_{\mathrm{CT}}(\infty) \rangle}{\langle \Delta E_{\mathrm{CT}}(0) \rangle - \langle \Delta E_{\mathrm{CT}}(\infty) \rangle}, \qquad (2)$$

where $\langle ... \rangle$ denotes an ensemble average. The resulting curve for PhPy in ACN is shown in Fig. 5. The initial dynamics ($0 \leqslant t \leqslant 200$ fs) is characterized by a rapid decay of $S(t)$ with a $1/e$ time of about 100 fs. At longer times there are two weak recurrences at $t = 300$ and 550 fs superimposed on a much slower decay with a picosecond timescale. The interpretation of this signal is based on an inspection of the underlying solvent dynamics: First there is an impulsive motion of the solvent particles in order to adjust to the change in the solute charge distribution. This motion extends beyond the new equilibrium geometry, oscillates back and so forth. However, the presence of dissipation in the solvent rapidly damps these oscillations.

The molecular dynamics simulations also allow one to identify the nature of the motion of the solvent particles on a microscopic scale. An investigation of radial distribution functions reveals that—due to the dense packing of molecules in the liquid—translational motions play only a minor role in the solvent response. Instead we investigate the rotational/librational motion of the solvent molecules. Fig. 6 shows the distributions of the angular reorientation of the solvent particles comprising the first solvation shell. This quantity is defined

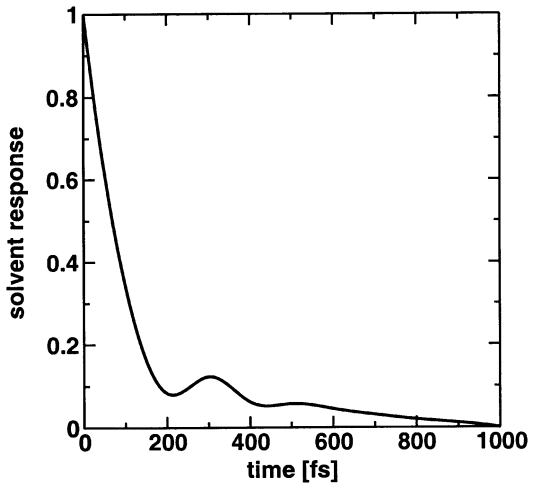

Fig. 5 Normalized dynamic Stokes shift characterizing the solvent response to instantaneous electronic excitation to the CT state, see eqn. (2).

as the change of the angle between the ACN symmetry axis and the vector from the center of mass of the ACN to the center of the nearer of the two rings (donor or acceptor). On the ultrashort timescale ($t = 100$ fs) the distribution function peaks between 5 and 15 degrees. After the decay of the oscillations of the solvent response, also larger reorientation angles up to 45 degrees are observed ($t = 1$ ps).

4 Conclusions

The real-time dynamics of electronically excited PhPy dissolved in ACN has been investigated using non-equilibrium molecular dynamics simulations. The interaction has been modeled by a combination of high level *ab initio* calculations for ground and several excited states of the solute and empirical potentials for the solvent. Two different contributions to the dynamic Stokes shift of the charge transfer state with respect to the locally excited state have been studied in detail, namely the intramolecular PhPy twisting and the ACN solvent rearrangement.

The resulting picture of the intramolecular dynamics of PhPy in ACN is that the solvent–solvent interaction is relatively strong compared with the solute intramolecular twisting torque of the CT state. In particular, the torsional motion of the solute towards perpendicularity can be slowed down to a large extent. In this way our simulations provide microscopic evidence of the viscosity of a polar solvent. Even though ACN does not form hydrogen bonds, the strong dipole–dipole interactions render ACN viscous enough to hinder the twisting motion connected with the intramolecular charge transfer.

The intermolecular dynamics of PhPy upon electronic excitation is characterized by the reorientation of the solvent to the change in the charge distribution of the solute. In particular, the stabilization of the CT state is responsible for the red-shift of the anomalous fluorescence. Thus, the simulated dual fluorescence confirms the validity of the TICT mechanism for PhPy in polar solution. In agreement with previous studies of other model solutes in ACN, the microscopic mechanism has been identified to be the orientational motion of the ACN molecules.[6] After an ultrashort period (≈100 fs) of free inertial rotation of the solvent particles, our simulations show weak recurrence structures indicating quasi-coherent librations. Indeed, the oscillatory structure of the corresponding normalized Stokes shift has been obtained experimentally for the first time for aminonitrofluorene solvated in ACN.[9] The very similar course of the solvent relaxation in our simulations suggests the interpretation that the oscillatory solvent response is rather a genuine feature of the ACN solvent and is—to a certain extent—independent of the choice of the solute.

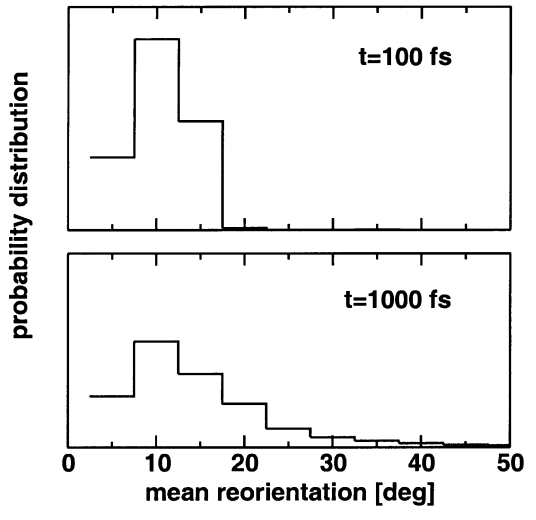

Fig. 6 Mean reorientation of ACN solvent molecules for selected times after instantaneous electronic excitation of PhPy to the CT state.

Acknowledgement

Financial support by the Volkswagen Foundation through grant I/75 908 (to B. Sch.) and by the Fonds der Chemischen Industrie (to J. M.) is acknowledged. Furthermore, the authors are grateful to Prof. W. Rettig and Prof. M. Merchan for helpful discussions.

References

1 J. Michl and V. Bonačić-Koutecký, *Electronic Aspects of Organic Photochemistry*, Wiley, New York, 1990.
2 E. Lippert, W. Lüder and H. Boos, in *Advances in Molecular Spectroscopy*, ed. A. Mangini, Pergamon, Oxford, 1962, p. 443.
3 Z. R. Grabowski, K. Rotkiewicz, A. Siemiarczuk, D. J. Cowley and W. Baumann, *Nouv. J. Chim.*, 1979, **3**, 443.
4 W. Rettig, in *Electron Transfer I*, ed. J. Mattay, *Topics in Current Chemistry*, vol. 169, Springer, Berlin, 1994, pp. 253–299.
5 D. Braun and W. Rettig, *Chem. Phys. Lett.*, 1997, **268**, 110.
6 M. Maroncelli, *J. Chem. Phys.*, 1991, **94**, 2084.
7 P. V. Kumar and M. Maroncelli, *J. Chem. Phys.*, 1995, **103**, 3038.
8 R. M. Stratt and M. Maroncelli, *J. Phys. Chem.*, 1996, **100**, 12981.
9 J. Ruthmann, S. A. Kovalenko, N. P. Ernsting and D. Ouw, *J. Chem. Phys.*, 1998, **109**, 5466.
10 W. Sudholt, A. Staib, A. L. Sobolewski and W. Domcke, *Phys. Chem. Chem. Phys.*, 2000, **2**, 4341.
11 W. Rettig and F. Marschner, *Nouv. J. Chim.*, 1983, **7**, 425.
12 H. Lumbroso, D. M. Bertin and F. Marschner, *J. Mol. Struct.*, 1988, **178**, 187.
13 K. Okuyama, Y. Numata, S. Odawara and I. Suzuka, *J. Chem. Phys.*, 1998, **109**, 7185.
14 B. Proppe, M. Merchan and L. Serrano-Andres, *J. Phys. Chem. A*, 2000, **104**, 1608.
15 A. B. J. Parusel, *Phys. Chem. Chem. Phys.*, 2000, **2**, 5545.
16 J. Manz, B. Proppe and B. Schmidt, *Z. Phys. D*, 1995, **34**, 111.
17 F. Evers, J. Giraud-Girard, S. Grimme, J. Manz, C. Monte, M. Oppel, W. Rettig, P. Saalfrank and P. Zimmermann, *J. Phys. Chem. A*, 2001, **105**, 2911.
18 A. L. Sobolewski, W. Sudholt and W. Domcke, *J. Phys. Chem. A*, 1998, **102**, 2716.
19 W. Sudholt, A. L. Sobolewski and W. Domcke, *Chem. Phys.*, 1999, **240**, 9.
20 W. Rettig and B. Zietz, *Chem. Phys. Lett.*, 2000, **317**, 187.
21 S. Hayashi, K. Ando and S. Kato, *J. Phys. Chem.*, 1995, **99**, 955.

22 K. Andersson, M. R. A. Blomberg, M. P. Fülscher, G. Karlström, R. Lindh, P.-Å. Malmqvist, P. Neogrády, J. Olsen, B. O. Roos, A. J. Sadlej, M. Schütz, L. Seijo, L. Serrano-Andrés, P. E. M. Siegbahn and P.-O. Widmark, *MOLCAS*, Version 4.0, Dept. of Theoretical Chemistry, Chemical Center, University of Lund, Sweden, 1997.
23 W. Domcke and G. Stock, *Adv. Chem. Phys.*, 1997, **100**, 1.
24 W. L. Jorgensen and T. B. Nguyen, *J. Comput. Phys.*, 1993, **14**, 195.
25 W. L. Jorgensen and J. M. Briggs, *Mol. Phys.*, 1988, **63**, 547.
26 M. P. Allen and D. J. Tildesley, *Computer Simulations of Liquids*, Clarendon, Oxford, 1987.
27 H. C. Andersen, *J. Comput. Phys.*, 1983, **52**, 24.
28 D. van der Spoel, A. R. van Buuren, E. Apol, P. J. Meulenhoff, D. P. Tieleman, A. L. T. M. Sijbers, B. Hess, K. A. Feenstra, E. Lindahl, R. van Drunen and H. J. C. Berendsen, *Gromacs User Manual version 3.1*, Nijenborgh 4, 9747 AG Groningen, The Netherlands, 2001, http://www.gromacs.org/.